Implementing 2-Qubit Quantum Computer via NMR

Muye "Willers" Yang*
MIT Department of Physics
(Dated: November 19, 2021)

In this experiment, we demonstrated quantum advantage with respect to query complexity through the Deutch-Jozsa algorithm and Grover's search algorithm on a two-qubit quantum computer implemented using liquid-state NMR techniques. Specifically, we show that certain problems can be solved using one query to an unknown function on our quantum computer, whereas any classical algorithms require at least two queries.

I. INTRODUCTION

Unlike the classic computation model, quantum computation relies on quantum systems as the basic unit of information, which are governed by laws of quantum mechanics. Quantum bits, or qbits, allow us access to additional computational primitives such as superposition, interference, and entanglement, and has the potential to solve certain mathematical problems such as factoring which are believed to be intractable classically.

However, despite the theoretical advancements, experimental demonstrations of quantum supremacy was not achieved until very recently [1], due to the difficulties in developing reliable quantum hardware. Under this constraint, quantum advantages are more often demonstrated in other metrics such as query complexity or space complexity[2]. In this experiment, we consider the query complexity to demonstrate quantum advantages on problems that can be solved with a 2-qubit quantum computer that we implement using techniques of liquid state NMR. We experimentally demonstrate that quantum algorithms can solve certain problems with strictly less queries than classical computers could, confirming the theoretical separation between classical and quantum query complexities.

We will begin with a brief introduction to quantum computation and and some of the details of how our quantum computers are implemented, including pure-state preparation, single qubit rotations, entangling gates, and pure-state preparation with the language of liquid-state Nuclear Magnetic Resonance (NMR). Then, we will define the algorithms of interest, the Deutch-Josza algorithm and Grover's search algorithm. Finally, we present the result of our implementation, and explores the oscillatory behaviours of Grover's search algorithm. Calibrations of our physical system and error analysis can be found in the appendix.

II. QUANTUM COMPUTING BASICS

A qubit, or a quantum bit, usually represents a two state system such as the magnetic-spin of a spin-1/2 particle. The state of these systems exhibit interesting quantum behaviours in the microscopic level, and can be manipulated according to laws of quantum mechanics.

Formally, we can represent a qubit by a normalized complex vector $|\psi\rangle = a|0\rangle + b|1\rangle$ in a two dimensional Hilbert Space $\mathcal{H}$, often referred to as the Bloch Sphere. In a two-qubit system, the composite state is the the tensor product of two qubits, or a normalized complex vector in the tensor product space $\mathcal{H}_1 \otimes \mathcal{H}_2$. $|0\rangle = [1,0]^T$ and $|1\rangle = [0,1]^T$ denote two basis states, and in the case of a spin-$\frac{1}{2}$ particle, they often denote the spin-up and spin-down state along the $\hat{z}$ direction. $|\psi\rangle$ is normalized s.t. $|a|^2 + |b|^2 = 1$. Qubits can be manipulated according to laws of quantum mechanics, which manifests as actions of unitary operators on the Hilbert space. Upon measurement of an observable Z, $|\psi\rangle$ collapses into a basis state of Z, $|0\rangle$ (or $|1\rangle$), with probability determined by the overlap $|a|^2$ (or $|b|^2$).

III. NMR IMPLEMENTATIONS

In our implementation of the 2-qubit quantum computer, we use the spins of H and C in chloroform ($^{13}CHCl_3$) solution as an ensemble of qubits, denoted $|HC\rangle$. At room temperature, the ensemble of qubits $|HC\rangle$ is approximately described by the density operator $\rho_{therm} \approx \frac{1}{4}I_{4\times4} + 10^{-4}\text{diag}\{5,3,-3,5\}$. To obtain a pure initial state $|00\rangle$ which is necessary to carry out any true quantum computation, we use the method of *time-averaging* over the cyclic relabeling of the last three eigenstates [3].

Using standard notations, we denote $R_x(\theta)$ and $R_y(\theta)$ as rotations by θ around $\hat{x}, \hat{y}$, which can be implemented on our physical qubits using pulsed NMR [4]. Let X, Y, Z denote the Pauli matrices, or the π rotation around $\hat{x}, \hat{y}$ and $\hat{z}$. Furthermore, the free evolution of the two spins over a time period t is characterized by a 2-qubit $Z \otimes Z$ interaction, $\tau(t) = \exp(\frac{i\pi Jt}{2} \cdot Z \otimes Z)$ where J is the coupling constant of H and C. For $t = 1/(2J)$, the effect of free evolution can be described by the unitary operator $\tau = e^{i\pi/4} diag\{-i, 1, 1, -i\}$.

In fact, $R_x(\theta), R_y(\theta)$ and the entangling gate τ make up a universal set of gates for quantum computation. That is, any quantum circuit can be decomposed into a circuit involving only $R_x(\theta), R_y(\theta)$ and τ. To show this,

* willers@mit.edu; http://willers.mit.edu

we can construct a famous universal set of gates, the Clifford+T gates:

$$H = R_x(\pi)R_y(\frac{\pi}{2}) \tag{1}$$

$$T = R_x(\frac{\pi}{4})R_y(\frac{\pi}{4}) \tag{2}$$

$$S = T^2 \tag{3}$$

$$CNOT = R_{y1}(-\frac{\pi}{2})\tau S_1 S_2 R_{x2}(-\frac{\pi}{2}). \tag{4}$$

Measurement on our qubits are done by applying a read-out pulse $R_x(\pi/2)$ to the qubit we're measuring, and then subsequently recording the response free induction decay (FID) of the total magnetization in the traverse plane. In the case of hydrogen, for an arbitrary state with density operator $\rho = \text{diag}\{a, b, c, d\}$, the spectrum of response FID (which we obtain through a FFT) will have a peak of area $a - c$ around $\omega_h - \frac{J}{2}$, and another peak of area $b - d$ around $\omega_h + \frac{J}{2}$, where ω_h is the Lamour frequency of hydrogen nucleus [5]. We plot the measured spectrum for $|00\rangle$ in figure 1 as an example.

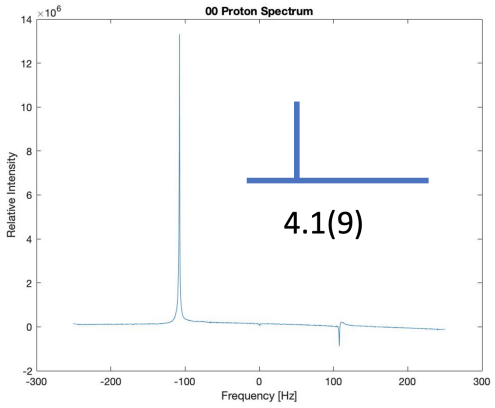

FIG. 1. Plot of the spectrum of Hydrogen's response FID. The ensemble of states measured is modeled by the pseudo-pure state $|00\rangle$ prepared via time-averaging. The peak integral of the left peak is $4.1(9) \times 10^5$. We represent this spectrum using a schematic drawn on the top right.

Specifically, we can use time-averaging to prepare the eigenstate $|00\rangle$, and prepare the remaining eigenstates $|01\rangle, |10\rangle, |11\rangle$ by applying $I \otimes X, X \otimes I, X \otimes X$ to $|00\rangle$. We perform a measurement on the four eigenstates and calculate the peak integral scaled by 10^5, giving us the following schematic representations of these spectrum in figure 2.

IV. EXPERIMENTAL RESULTS

We carry out two experiments on our 2-qubit quantum computer, one implementing the Deutsch-Jozsa Algorithm to solve a decision problem on boolean functions, and the other implementing Grover's Algorithm for the static search problem. The Deutsch-Jozsa Algorithm, although of little practical use, is an important theoretical result, since it provides an oracle separation between the classical complexity class **P**, the set of problems that can be solved efficiently (in polynomial time) on a classical computer, and the quantum analogue **EQP**, the set of problems that can be solved exactly in polynomial time on a quantum computer.

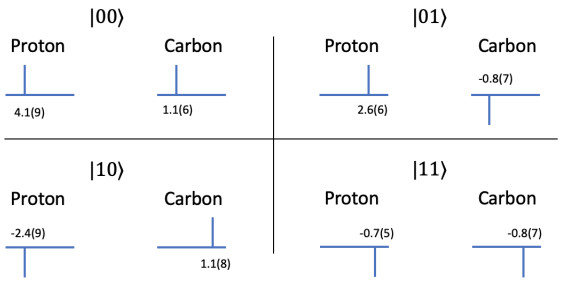

FIG. 2. Schematics of the spectrum of each pure state. The number below the schematics represent the area under the largest peak, scaled by 10^5.

IV.1. Deutsch-Jozsa Algorithm

The problem Deutsch-Jozsa algorithm is developed to solve is formulated as follows: Given an unknown boolean function f, which takes an input x, an n-bit string, and outputs either 0 or 1. Suppose we are promised that f is either constant ($f(x) = f(y) \forall x, y \in \{0,1\}^n$) or it is faithful ($|\{x : f(x) = 0\}| = |\{x : f(x) = 1\}|$). That is, f is constant if it maps all inputs to the same output, or it is faithful if it maps exactly half of the inputs to 0 and the other half to 1. In the quantum analogue of this problem, f is encoded as a unitary operator U_f, which stores the value of the computation onto a work qubit: $U_f |x\rangle \otimes |0\rangle = |x\rangle \otimes |0 \oplus f(x)\rangle$. In particular, there are four boolean functions on inputs on length 1. The quantum oracle for these functions can be constructed via NMR pulses as listed in table I. We note that f_1, f_2 is constant, and f_3, f_4 is faithful.

	f_1	f_2	f_3	f_4
Classical	$0 \to 0$	$0 \to 0$	$0 \to 0$	$0 \to 0$
Mapping	$1 \to 0$	$1 \to 0$	$1 \to 0$	$1 \to 0$
U_f	I	X^c	$CNOT$	$X^c CNOT$

TABLE I. The four boolean functions with input of length 1 and their corresponding quantum oracles U_f.

Classically, more than half of the input needs to be evaluated in the worst case before we can determine whether a function f is constant or faithful. For input strings of length n, this is $O(2^n)$ queries to the function f. Surprisingly, in the quantum analogue, one query to

U_f suffices to determine whether f is constant or faithful. We now describe how the problem is solved on a two-qubit quantum computer. We allocate one qubit as the work qubit initialized to $|0\rangle$, and the other qubit as our input string of length 1 also initialized to $|0\rangle$. Let $U_1 = R_y(-\frac{\pi}{2}) \otimes R_y(\frac{\pi}{2})$ and $U_2 = U_1^{-1} = R_y(\frac{\pi}{2}) \otimes R_y(-\frac{\pi}{2})$. Then, on input function f, we can run the circuit composed of one U_f, $U_2 U_f U_1 |00\rangle$, which returns:

$$U_2 U_f U_1 |00\rangle \tag{5}$$
$$= U_2 U_f \frac{1}{2}[|0\rangle + |1\rangle] \otimes [|0\rangle - |1\rangle] \tag{6}$$
$$= U_2 \frac{1}{2}[(-1)^{f(0)} |0\rangle + (-1)^{f(1)} |1\rangle] \otimes [|0\rangle - |1\rangle] \tag{7}$$
$$= \frac{1}{2}[\alpha_f |0\rangle + \beta_f |1\rangle] \otimes |0\rangle . \tag{8}$$

where in line 8, $\alpha_f = ((-1)^{f(0)} + (-1)^{f(1)})$, $\beta_f = (-(-1)^{f(0)} + (-1)^{f(1)})$. Note, when f is constant, $f(0) = f(1)$, $\alpha_f = \pm 1$ and $\beta_f = 0$, giving us the final output $\pm |00\rangle$. When f is faithful, $f(0) \neq f(1)$, $\alpha_f = 0$ and $\beta_f = \pm 1$, giving us the final output $\pm |10\rangle$. Therefore, with one query to U_f, we can determine whether f is constant or faithful, depending on whether the final output is $\pm |00\rangle$ or $\pm |10\rangle$, whereas classically we must query f twice on input 0 and 1 to make a decision.

We run the aforementioned circuit on all four functions, and report the resulting spectrum and peak integral for f_3 (faithful function) in figure 3. The results for other functions can be found in appendix C.

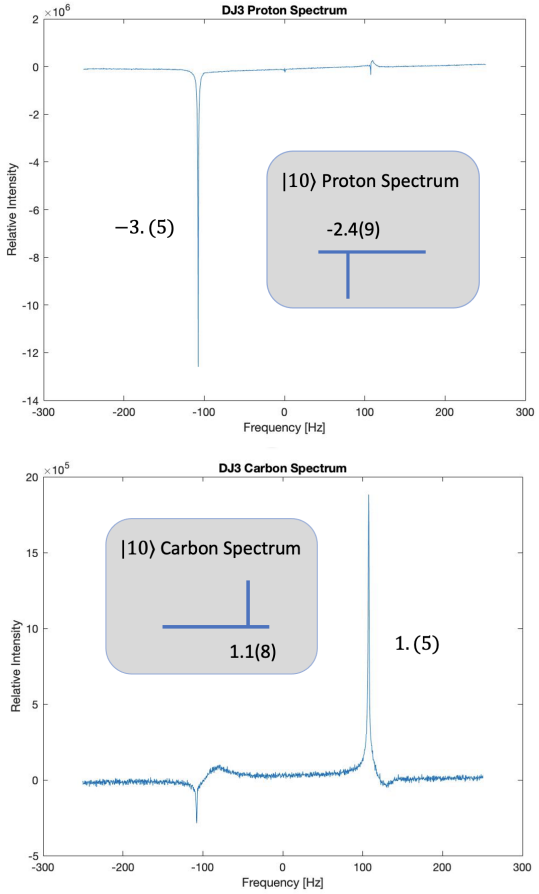

FIG. 3. Measured spectrum compared against the expected spectrum of state $|10\rangle$. We see that the observed peak integral matches with expected peak integral values.

IV.2. Grover's Search Algorithm

Despite its theoretical importance, the Deutsch-Jozsa algorithm currently have little practical use. Indeed, the promise of functions being constant or faithful does not arise naturally, and even when the promise is given, simple random sampling solves the problem efficiently and fails with probability that decreases exponentially with each additional query.

We turn to the problem of static search, which is a practical problem whose worst case run time on a Quantum Computer is polynomially better than the expected run time on a classical computer. The problem is formulated as follows: given a boolean function f which recognizes a hidden variable x_0 (that is, $f(x_0) = -1$, and $f(x) = 1$ otherwise), we wish to uncover x_0. The best randomized algorithm evaluates f at x chosen uniformly at random; the expected number of queries needed is $\frac{n+1}{2} = O(n)$.

In the quantum analogue of the problem, f is again encoded in a unitary function U_f s.t. $U_f |x_0\rangle = -|x_0\rangle$, and $U_f |x\rangle = |x\rangle$ for all other $x \neq x_0$. The quantum static search problem can be solved using Grover's search algorithm with only $O(\sqrt{n})$ queries to U_f. For a given f which recognizes x_0 and its quantum operator U_f, we can construct the Grover's oracle $G = H^{\otimes 2} P H^{\otimes 2} U_f$, where $P = 2|00\rangle\langle 00| - I$ is a special phase operator.[1] We can consider the action of G on an initial state ψ geometrically. Let $|\alpha\rangle = \sum_{x \neq x_0} |x\rangle$ (up to normalization) be the state composed of all non-solutions, and $|\beta\rangle = |x_0\rangle$ be solution state. Then, our initial state can be written as $|\psi\rangle = \sqrt{\frac{n-1}{n}} |\alpha\rangle + \sqrt{\frac{1}{n}} |\beta\rangle$. Define the angle between $|\psi\rangle$ and $|\beta\rangle$ to be $\frac{\theta}{2}$, where $\sin(\frac{\theta}{2}) = \sqrt{\frac{1}{n}}$. Then, the operation of U_f on $|\psi\rangle$ is a reflection about $|\beta\rangle$: $U_f |\psi\rangle = \sqrt{\frac{n-1}{n}} |\alpha\rangle - \sqrt{\frac{1}{n}} |\beta\rangle$; and the action of $H^{\otimes 2} P H^{\otimes 2} = (2 \sum_x |x\rangle\langle x| - I)$ is a reflection of $U_f |\psi\rangle$ around the original state $|\psi\rangle$. Overall, the action of G on $|\psi\rangle$ rotates $|\psi\rangle$ by angle $\theta = 2\sin^{-1}(\frac{1}{\sqrt{n}})$ towards the solution state $|\beta\rangle$: $G|\psi\rangle = \cos\frac{3\theta}{2} |\alpha\rangle + \sin\frac{3\theta}{2} |\beta\rangle$. This process is illustrated in figure 4 from [6]. Clearly, we will uncover the solution state $|x_0\rangle = |\beta\rangle$ after $O(\sqrt{n})$ iterations, which is polynomial faster than the classical

[1] Note U_{00} (constructed later) and P are equivalent up to an undetectable global phase.

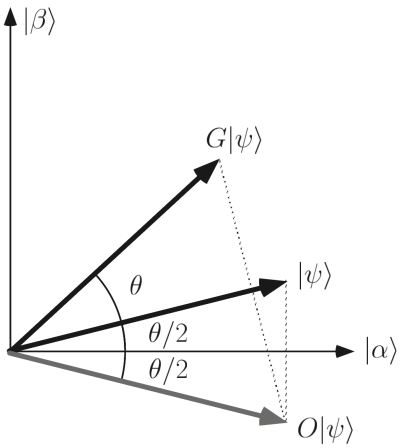

FIG. 4. The action of Grover's oracle G on a state $|\psi\rangle$, where $O = U_f$ denote the operator that recognize the solution state $|\beta\rangle$.

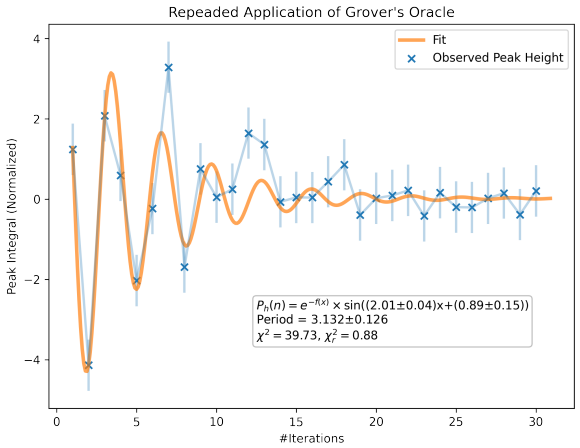

FIG. 5. Plot of the peak integral of Hydrogen's spectrum of state $G^k H |00\rangle$, with $|x_0\rangle = |00\rangle$. After one iteration, a local maximum is achieved, corresponding to the recovery of $|x_0\rangle$. The peak amplitude exhibit an oscillatory behaviour with period 3.132 ± 0.126 iterations, confirming the prediction by equation 10.

algorithm.

Furthermore, we see that in general,

$$G^k |\psi\rangle = \cos(\frac{2k+1}{2}\theta) |\alpha\rangle + \sin(\frac{2k+1}{2}\theta) |\beta\rangle ; \qquad (9)$$

and, the amplitude $\langle x_0| G^k |\psi\rangle = \sin(\frac{2k+1}{2}\theta)$ oscillates with angular frequency $\theta = 2\sin^{-1}(\frac{1}{\sqrt{n}})$.

In particular, with inputs of length 2, there are four possible f with the hidden variable $x_0 \in \{00, 01, 10, 11\}$. To find U_{11}, the unitary operator that recognizes $x_0 = |11\rangle$, we notice that $U_{11} = \text{diag}\{1, 1, 1 - 1\} = CZ$, where CZ denote the controlled Z gate. Using the conjugation rule $HXH = Z$, we have that

$$U_{11} = CZ = I \otimes H \cdot CNOT \cdot I \otimes H, \qquad (10)$$

where $CNOT$ and H can be implemented using pulses 1 and 4. Furthermore, we can obtain U_{00}, U_{01}, U_{10} (up to a global phase) by applying $Z \otimes Z$, $I \otimes Z$ and $Z \otimes I$ to U_{11}.

Classically, the expected number of queries needed is 2.5. However, if we start with the fully mixed state (up to normalization) $|\psi_0\rangle = \sum_{x=00}^{11} |x\rangle = H^{\otimes 2} |00\rangle$, then exactly one iteration of the Grover's Oracle is needed to recover the initial state x_0. We apply G^k to $|\psi_0\rangle$ for $k = 1, 2, ..., 50$ for each function f with $x_0 = \{00, 01, 10, 11\}$, and report the resulting amplitude for $|x_0\rangle = |00\rangle$ over the first 30 iterations in figure 5. For $n = 4$, $\theta = 2\sin^{-1}\frac{1}{2} = \frac{\pi}{3}$, which means that the relative amplitude should show an oscillatory behaviour of period 3 iterations. According to the fit of a decaying sin wave to our observed data, we obtain an empirical oscillatory period of $3.132 \pm 0.126 \approx 3$ iterations, as expected.

V. CONCLUSION AND FUTURE WORKS

In this report, we successfully implemented the Deutch-Josza algorithm and Grover's search algorithm for two problems on boolean functions, using exactly one query to an unknown boolean function, whereas the (expected) number of queries needed on a classical computer is 2 and 2.5 respectively. The result of our implementations confirms that quantum computers have an advantage over classical computers with respect to query complexity on certain problems.

The demonstrated advantage for query complexity should not be confused with a more general time advantage. Our results should be interpreted as a proof of concept rather than a practical improvement. In fact, liquid state NMR quantum computers are not good candidates for demonstrating a time advantage. As a reminder, to obtain a pseudo-pure state using time-averaging, three repetitions separated a sufficiently long waiting time t_w is required for each measurement. The wait time t_w is necessary to ensure that the perturbed state rethermalizes, and is proportional with the relaxation times T_1. On one hand, we need long T_1 time so the qubits persistent long enough for computation, while on the other hand, a long T_1 time also increases the run time. The run time of our quantum algorithm comes with the overhead cost of $3t_w$, which in our case is to the order of minutes! Liquid state NMR quantum computers, however, could be a good candidate for demonstrating other types of quantum advantages whose evaluation methods are based on success probability or circuit size. One possible direction is to consider quantum space advantage, which is recently demonstrated experimentally in [2].

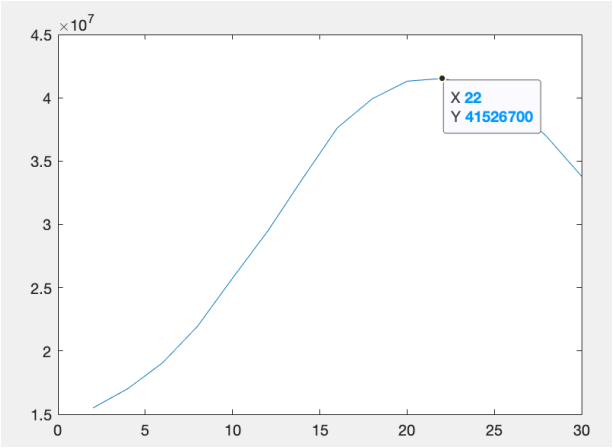

FIG. 6. Plot of the total FID response over pulse width [ms] for Carbon. We determine that $t_{90}^c = 22 \pm 0.5$[ms]

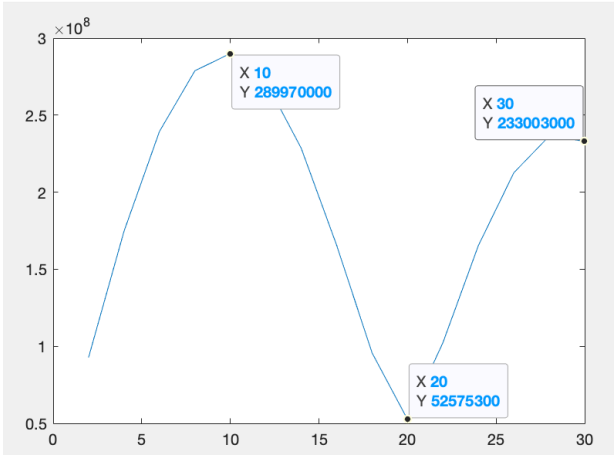

FIG. 7. Plot of the total FID response over pulse width [ms] for Hydrogen. We determine that $t_{90}^h = 10 \pm 0.5$[ms]

[1] F. Arute, K. Arya, R. Babbush, D. Bacon, J. Bardin, R. Barends, R. Biswas, S. Boixo, F. Brandao, D. Buell, B. Burkett, Y. Chen, Z. Chen, B. Chiaro, R. Collins, W. Courtney, A. Dunsworth, E. Farhi, B. Foxen, and J. Martinis, Nature **574**, 505 (2019).

[2] D. Maslov, J.-S. Kim, S. Bravyi, T. J. Yoder, and S. Sheldon, Nature Physics **17**, 894–897 (2021).

[3] D. Cory, R. Laflamme, E. Knill, L. Viola, T. Havel, N. Boulant, G. Boutis, E. Fortunato, S. Lloyd, R. Martinez, and et al., Fortschritte der Physik **48**, 875–907 (2000).

[4] M. Yang, "Measuring t_2 of diluted glycerin as a function of concentration," .

[5] *Quantum Information Processing with NMR*, MIT Junior Lab (2015).

[6] M. A. Nielsen and I. L. Chuang, *Quantum Computation and Quantum Information: 10th Anniversary Edition* (Cambridge University Press, 2011).

Appendix A: Calibrations

We determine the 90 degree pulse width for carbon and hydrogen by trying 30 different pulse widths $1, 2, ..., 30$ [ms] and choosing the first pulse width that maximizes the total FID response, as measure by the numerical integration of the absolute value of the response FID. We determine $t_{90}^h = 10 \pm 0.5$[ms], and $t_{90}^c = 22 \pm 0.5$[ms]. See figure 6 and 7 for reference.

We determine $J = 215 \pm 1$[Hz] by taking the difference between the two peaks in the measured spectrum, $\omega_h = 200.13(5)$[MHz] and $\omega_c = 50.33(5)$[MHz] by taking the mid-point of the two peaks in the measured spectrum.

Appendix B: Error Analysis

The uncorrelated, statistical errors that comes with fitting and averaging is accounted for in the uncertainty of the reported fit parameters. For the remainder of this section, we will discuss other main sources of systematic errors and how they are incorporated in our analysis.

First, the numerical scheme we chose for finding the peak integral is the simple mid-point method, which we estimate to contribute up to 10% relative error for the peak integrals. The specific uncertainties are reported with our results. We obtain these estimations by applying our numerical scheme to the background noise, and comparing the integral of the noise to the peak integral of the signal. We choose to use a numerical integral scheme rather than fitting a Lorenzian function since the spectrum we obtain is often asymmetric, prohibiting a reasonable fit.

Secondly, the pulse width t_{90} carbon and hydrogen is obtained by maximizing the total response FID (numerical integral of the absolute value of the FID) for 30 test values $1, 2, ..., 30$ [ms]. Note since the resolution is only 1 [ms], our estimation of t_{90}^h and t_{90}^c comes with an uncertainty of ± 0.5 [ms], which is more than 5% of t_{90}^h. The precision of t_{90} determines the precision of our quantum algorithms, since all of our gates are built using 90-pulses. Furthermore, the uncertain could also propagate with each additional gate built using this t_{90}. We account for this by increasing the uncertainty of the peak integral by a multiplicative factor of $0.5/10 = 5\%$ for hydrogen and $0.5/22 \approx 2\%$ for carbon, for each rotation by $\pi/2$. For the Deutzh-Josza's algorithm, this comes out to be $\approx 20\%$ for hydrogen, and $\approx 10\%$ for carbon, which is why the reported uncertainty is in some cases larger for the peak integrals of the Deutsch-Josza outputs than those of the pure states. For Grover's algorithm, we see

that this results in an exponential decay of the resulted amplitude characterized by $T \approx 0.3\text{s} \ll T_1, T_2$.

Appendix C: More Deutch-Jozsa Results

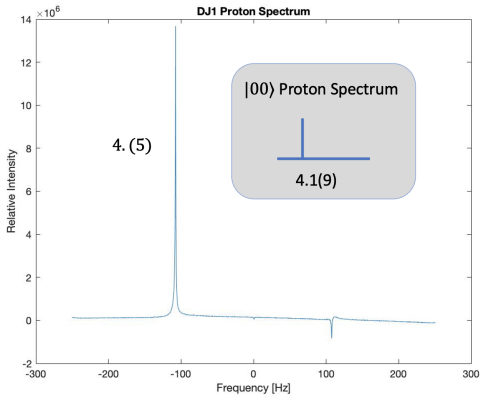

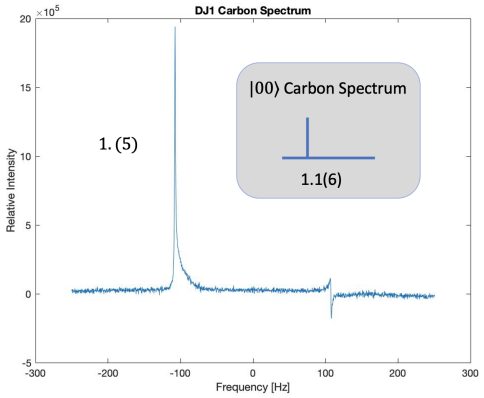

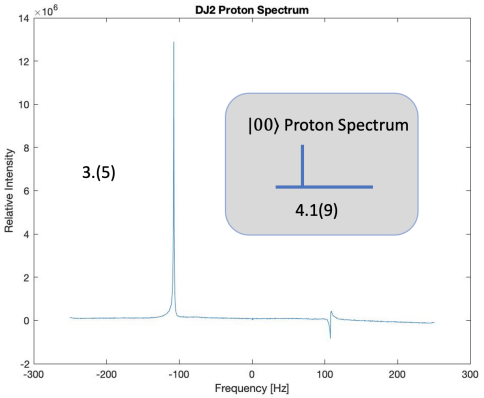

Appendix D: Acknowledgement

We thank Xiaoyang Zhuang for her partnership and help with calibrations. We also thank Junior Lab staff for their helpful suggestions and their support with trouble shooting.